Available online at www.sciencedirect.com
SCIENCE DIRECT®
Methods 31 (2003) 306–316
METHODS
www.elsevier.com/locate/ymeth

Focused microarray analysis

Elisa Wurmbach,[a] Tony Yuen,[a] and Stuart C. Sealfon[a,b,c,*]

[a] Department of Neurology, Mount Sinai School of Medicine, Box 1137, 1 Gustave L. Levy Place, New York, NY 10029, USA
[b] Fishberg Research Center for Neurobiology, Mount Sinai School of Medicine, New York, NY 10029, USA
[c] Department of Pharmacology and Biological Chemistry, Mount Sinai School of Medicine, New York, NY 10029, USA

Accepted 25 April 2003

Abstract

We describe detailed protocols and results with an integrated platform for studying relative transcript expression, including microarray design and fabrication, analysis and calibration algorithms, and high throughput quantitative real-time PCR. This approach optimizes sensitivity and accuracy while controlling the cost of experiments. A high quality cDNA array was fabricated using a restricted number of carefully selected transcripts with each clone printed in triplicate. This focused array facilitated both repeated measurement and replicate experiments. Following normalization and differential expression analysis, we found that experiments with this array identified differentially expressed transcripts with a high degree of accuracy and with high sensitivity to low levels of differential expression. Using a calibration algorithm improved the accuracy of the array in quantifying the relative level of transcript expression. All differentially expressed transcripts identified by the array were independently tested using high throughput quantitative real-time PCR assays. This approach reliably identified transcripts having as low as 1.3-fold differences in transcript expression between RNA samples from treatment- and control groups and was applicable to highly heterogenous tissue sources such as hypothalamus and cerebral cortex.
© 2003 Elsevier Inc. All rights reserved.

Keywords: Microarray; Real-time PCR; Sensitivity; Specificity; Quality control; Validation; Fluorescence; cDNA; Calibration; Normalization

1. Introduction

Studying transcript expression in a massively parallel fashion has rapidly become an essential component of modern biological research. The rapid implementation of these various technologies can be appreciated by searching PubMed between 1996 and 2002 for the term "microarray." The number of publications increased exponentially from two in 1996 to 1465 in 2002. Although microarrays have become widely used, generally accepted standards for data reproducibility and reliability have not yet been established. The parallel measurement of transcript expression actually consists of diverse measurement and analysis approaches (reviewed in [1]). We describe an integrated microarray and validation platform developed in our laboratory, called focused microarray analysis (FMA), that we find confers advantages in terms of reproducibility, cost effectiveness, and measurement accuracy.

The objective of a microarray experiment is to take RNA samples from an experimental paradigm and to correctly identify transcripts that are differentially expressed between groups. If the goal is to be attained efficiently, the various components that affect this process must be optimized and integrated. The reduction of measurement variability at all stages in the microarray experiment is important for improving the outcome (see also [2]). The controllable sources of error in microarray experiments include the biological procedure, RNA isolation, labeling method, microarray fabrication, hybridization conditions, and analysis algorithms. The major elements to consider, all of which contribute to the success of the experiment, are presented schematically in Fig. 1.

Several attributes are desirable in any microarray platform. The microarray should have a high sensitivity

* Corresponding author. Fax: 1-212-289-4107.
E-mail address: Stuart.Sealfon@mssm.edu (S.C. Sealfon).

1046-2023/$ - see front matter © 2003 Elsevier Inc. All rights reserved.
doi:10.1016/S1046-2023(03)00161-0

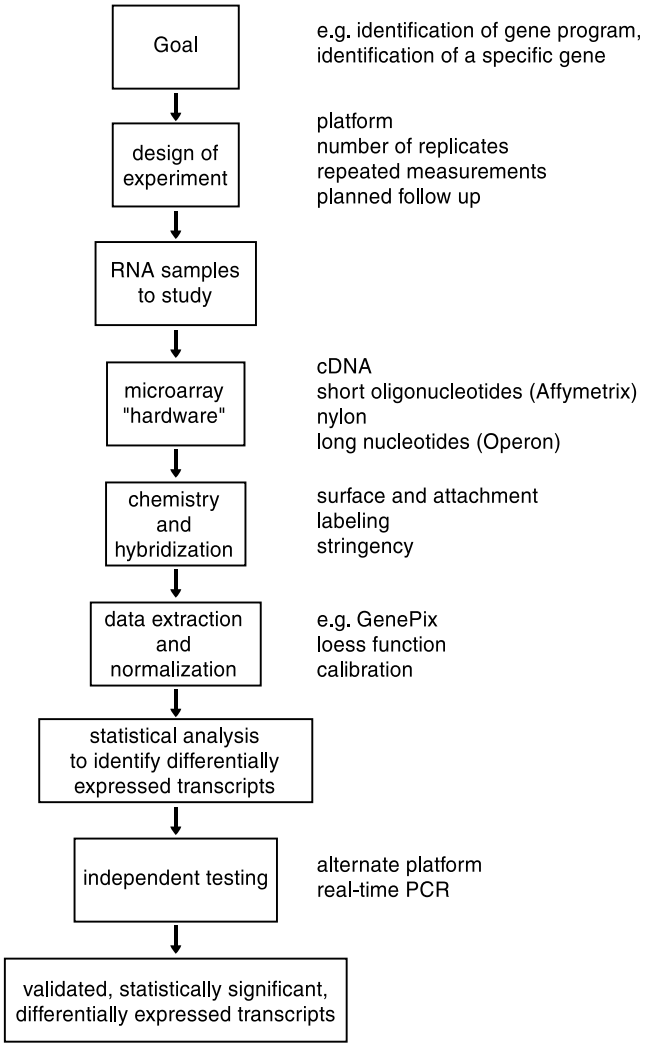

Fig. 1. The major components of a microrray-based experiment are illustrated.

for identifying differentially expressed transcripts, including transcripts that have a low level of expression and/or relatively low degree of differential expression. In addition, a low false positive rate (specificity) is desired. The usefulness of the microarray experiment decreases as the percentage of unregulated transcripts that are falsely identified as regulated increases. Additional features desirable in a microarray platform are the capacity to simultaneously evaluate as many transcripts as possible, determined by the number of transcripts assayed on the array ("coverage"), and to complete the experiment at the lowest cost and least effort possible.

However, many of the desirable attributes of a microarray platform are to a considerable extent mutually exclusive. There is a trade-off between specificity and sensitivity. As the threshold for identifying regulated transcripts is decreased, the false positive rate must increase. There is a trade-off between coverage and both cost and specificity. Because of the statistical issue of error control with multiple hypothesis testing, increasing the number of transcripts assayed on the array must either increase the false positive rate or decrease the sensitivity [3]. Increasing the number of replicate experiments increases the accuracy and sensitivity, but also increases the cost of the experiment and the work involved in preparing the samples for analysis.

The design of a microarray experiment should be tailored to its specific objectives. In general, there are two goals of a microarray experiment. (1) Microarrays can be used to identify a specific unknown transcript that confers a particular biological function. For example, a particular receptor may be expressed in one cell of a tissue source but not in another, and a microarray could be used to identify gene candidates for that receptor based on differential expression. In this case, the experiment will succeed only if the array contains this particular receptor gene, and, therefore, complete genome coverage may be desirable. (2) More commonly, microarrays are utilized to identify and to study a gene program. Examples include the identification of tumor subtype specific markers, studies of cell cycle genes, or studies of the activation of a gene program by a hormone. In this type of experiment, assaying a defined collection of transcripts may be preferable.

The scale of genome-wide microarrays introduces several problems. One is the difficulty of quality control for both academic and commercial suppliers. In addition, the high expense of global arrays constrains the number of arrays that can be analyzed to provide statistically acceptable sensitivity and specificity. Therefore, as an alternative, we developed FMA, in which the array contains a selection of genes that are printed in triplicate. Although FMA provides less broad transcriptome coverage than a global array, this limitation can be partially overcome by the careful selection of clones which are represented. We find that FMA facilitates the generation of high quality experiments and is sensitive to small regulatory changes that can be confirmed by independent measurements. This approach provides an adaptable solution to the relative optimization of a microarray experiment designed to identify and study a gene program.

We describe here in detail the development of FMA including the fabrication of a high quality custom-made cDNA microarray followed by independent QRT-PCR. In addition, we demonstrate the performance of FMA in varied applications, including experiments in a cell-line, hypothalamus, and cortex. We also assess the limitations in studying differentially expressed transcripts in complex tissues.

2. Development of an early gene cDNA microarray

The fabrication of a custom-made focused cDNA microarray entails the careful selection of genes, PCR

amplification and purification, printing onto slides, and the attachment of these products to slides.

2.1. Selection of genes

The gene selection for our array was based on literature searches and input from collaborating laboratories. Included were a large number of genes known to be induced at early time points in other experiments as well as 67 ''housekeeping'' genes. Nine hundred and fifty six clones were selected for printing, including 696 cDNAs from the National Institute of Aging 15K mouse library [4], 181 cDNAs purchased from Research Genetics, and 79 clones from individual laboratories [5]. The number of genes selected for printing was limited to roughly 1000 in order to facilitate handling and verification. This group included all genes of interest identified and an adequate number of unregulated genes to allow subsequent data normalization.

2.2. Amplification and purification

Plasmids were purified using the Qiaprep 96 Turbo Miniprep kit (Qiagen, Valencia, CA). Following the amplification of inserts by PCR, product size, and specificity were confirmed by agarose gel electropheresis. As the total number of products amplified was manageable, each product could be checked and PCR repeated under different conditions, if necessary. The products were purified with Qiaquick 96 kit (Qiagen, Valencia, CA).

The accuracy of the libraries utilized contributes to the quality of the platform. Confirming all clones printed by sequencing provides the highest accuracy, however this can be time consuming and expensive. We verified the picked clones to determine library accuracy. One hundred fifty four clones printed on the array which included randomly selected ones in each 96-well plate and all genes that were identified as regulated in LβT2 cell line experiments were sequenced [5]. Ninety-six percent of the clones picked from NIA library and 84% from the clones purchased from Research Genetics had been correctly identified. All clones received from other sources were sequence confirmed. Based on the distribution of clone sources, we estimate that 94% of the clones on the array were correctly identified.

2.3. Attachment of PCR products to glass slides

We used the GMS 417 Arrayer (Affymetrix, Santa Clara, CA) to print the amplified clones. Suspension solutions and fixing protocols were compared in a 3×3 factorial design. Feature morphology is influenced by surface tension effects arising from surface material, spotting solution chemistry, and by attachment efficiency [6]. Several inserts of varying size were utilized for this experiment. The purified PCR products were dried and dissolved in either 18 μl H_2O, 18 μl of 50% DMSO or 18 μl of 3× SSC and spotted using three hits per feature on CMT-GAPS coated glass slides (Corning, Corning, NY). DNA was fixed either by incubating the slide for 3.5 h at 40 °C followed by 10 min at 100 °C or for 2 h at 85 °C or by UV cross-linking with 90 mJ (Stratalinker, Stratagene, La Jolla, CA).

The feature morphology and attachment were evaluated by hybridizing a small test array with a Cy5-labeled oligonucleotide (Integrated DNA Technologies, Coralville, IA) complementary to one of the amplification primers (5′-CGT TTT ACA ACG TCG TGA CTG GG-3′). The hybridization with the oligonucleotide was performed at low stringency. Fifty nanograms of labeled oligonucleotide was diluted in 12 μl of 50% formamide, 6× SSC, 0.5% SDS, and 5× Denhardt's with 1.2 μg of salmon sperm DNA. The test arrays were pre-hybridized in 6× SSC, 0.5% SDS, and 1% BSA for at least 45 min at 42 °C. After washing the slides with water, the labeled oligonucleotide was hybridized in a humid chamber for 16 h at room temperature, followed by 5 min washes in 0.1× SSC, 0.1% SDS, twice in 0.1× SSC, and a short rinse in water. The slides were scanned using the GMS 418 Scanner (Affymetrix, Santa Clara, CA).

Fig. 2 shows the results from one optimization experiment. DNA dissolved in 3× SSC caused ring artifacts, seen in the right column. Attachment by two stage heating or by UV cross-linking was inconsistent, as seen in the top two rows. The optimum morphology and intensity were reproducibly observed, independently of insert sequence or size, with the PCR product dissolved in 50% DMSO and fixed for 2 h at 85 °C to CMT-GAPS coated slides. Based on these test experiments, all purified 956 PCR products were dissolved in 50% DMSO and slides were fixed for 2 h at 85 °C after printing.

All products were spotted in triplicate. This allows three repeated measures of each transcript on each slide, a capability that facilitates the distinction of hybridization signal from surface artifacts and provides the basis for the data analysis algorithm, which we implemented.

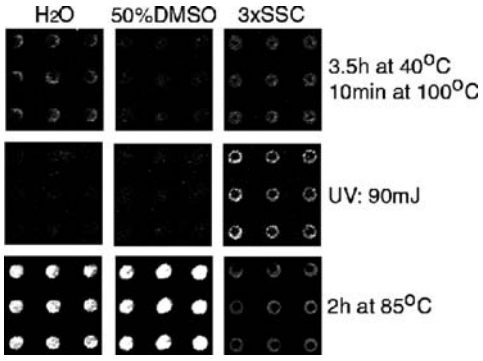

Fig. 2. Comparison of spotting solutions and attachment protocols. Reprinted from [5], with permission of the publisher.

The cDNA microarrays were stored in the dark at room temperature until use. A test hybridization with the Cy5-labeled oligonucleotide revealed that all PCR products were printed and attached (Fig. 3).

2.4. Probe labeling and hybridization

We preferred indirect probe labeling techniques, because direct incorporation of fluorophore-modified nucleotides has been reported to be associated with sequence-specific incorporation bias [7]. For incorporation of fluorophore in the cDNA synthesized from RNA samples, we used the Atlas indirect labeling kit (Clontech Laboratories, Palo Alto, CA). About 10–20 μg of total RNA was either labeled with Cy5 or Cy3 following the manufacturer's instructions.

Hybridization using cDNAs was performed under high stringency: pre-hybridization was at 42 °C in 6× SSC, 0.5% SDS, and 1% BSA for at least 45 min. Prior to hybridization, the Cy5- and Cy3-labeled cDNA samples were combined and diluted in 24 μl of 50% formamide, 6× SSC, 0.5% SDS, 5× Denhardt's with 2.4 μg salmon sperm DNA, and 10 μg poly(dA). After rinsing the array with water, the denaturated probe was hybridized at 42 °C in a humid chamber for at least 16 h. Following 10 min washes in 0.1× SSC, 0.1% SDS, twice in 0.1× SSC, and rinsing in water the slide was dried by spinning and scanned at 532 nm (Cy3) and 635 nm (Cy5) using the GMS 418 Scanner (Affymetrix, Santa Clara, CA). An overlay of the raw TIFF files of both channels is shown in Fig. 4. Triplicate spotting makes it easy to identify artifacts (see Fig. 4D).

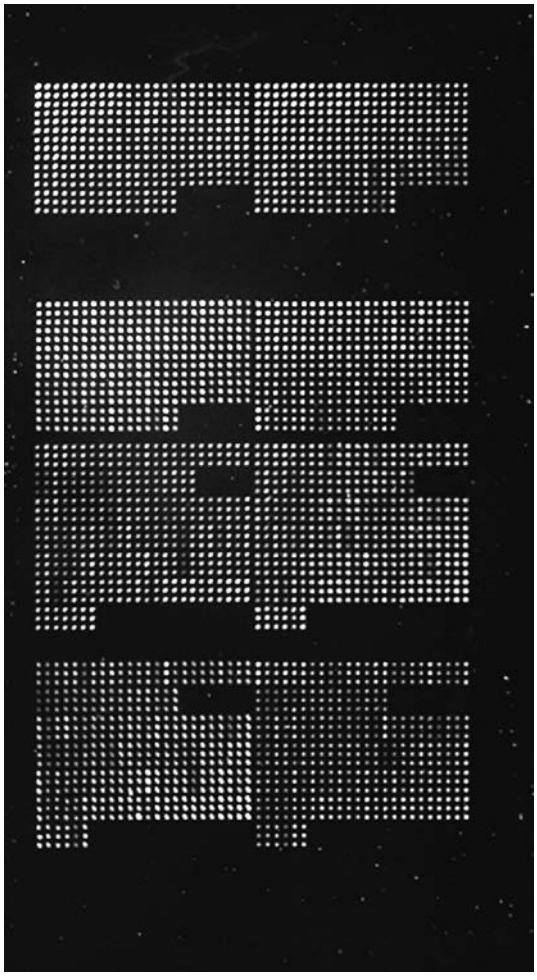

Fig. 3. Hybridization with a Cy5-labeled oligonucleotide that recognizes the priming site used for PCR amplification, to visualize all clones spotted on the array. All clones spotted are visible. Reprinted from [5], with permission of the publisher.

2.5. Dye reversal experiment

Fig. 5 shows the scatter plots obtained from two experiments in which the same cDNA samples were hybridized with the Cy3 and Cy5 labeling reversed. Some regulated triplicate genes are encircled, using the same color for the same gene in both plots. The correlation of the regulated genes is very high, $r = 0.975$. These results confirm that the indirect labeling avoids sequence-specific incorporation biasing.

2.6. Measurement and experimental reproducibility

When identical RNA samples (from control and treatment groups) were labeled repeatedly, a high correlation was obtained for the ratios of the regulated genes ($r = 0.985$), indicating that the data produced by this microarray are highly reproducible. We also compared the array results obtained in three independent experiments obtained from a gonadotrope cell line exposed to gonadotropin releasing hormone or vehicle (Fig. 6). We found that the differential expression observed was reproducible across different experiments and different arrays, indicating that satisfactory control of both experimental and measurement variation had been achieved ($r = 0.974$).

2.7. Data analysis

The TIFF-files generated from the GMS Scanner were imported into Genepix (Axon Instruments, Union City, CA). The spot identification was corrected manually, as suggested by the manufacturer, and the median background-subtracted signal intensity was utilized for further analysis.

2.7.1. Normalization

Overall differences in the signal intensity of the two wavelengths measured on each slide (at 532 and 635 nm) were corrected using the loess function, a locally linear robust scatter plot smoother, contained in S Plus Professional (Insightful, Seattle, WA). We preferred this normalization to an overall linear correction because it

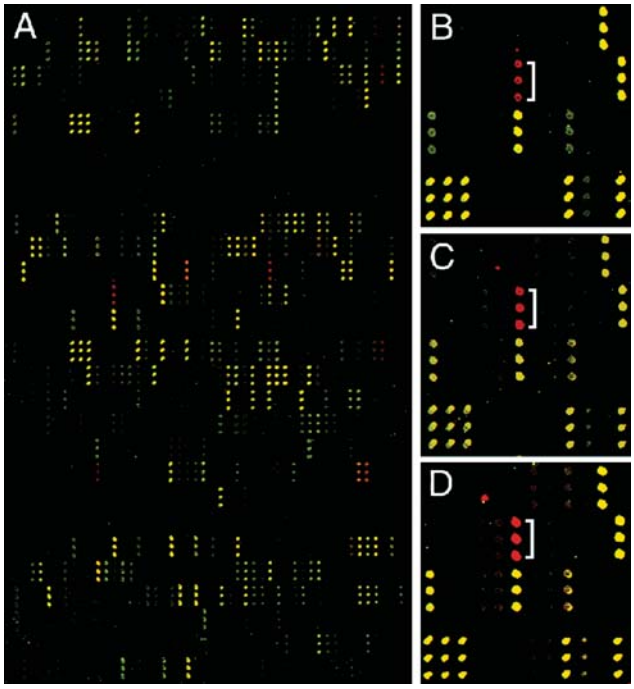

compensates for variation of the correction factor with signal intensity and is largely unaffected by outliers, including the regulated transcripts. Most transcripts were not regulated and the normalized data were tightly grouped along $y = x$. Predictors were generated using a symmetric distribution, span = 0.75.

2.7.2. Identification of differentially expressed transcripts

Three criteria were evaluated in order to identify the differentially expressed candidate genes using data from replicate experiments: the fold-change, the *t* statistic calculated within each slide from the repeated measurements on each slide, and the signal intensity. A gene was considered differentially expressed in the samples compared on a single array if all three criteria were satisfied:

(A) Fold-change: absolute value of the fold-change >1.3.

(B) *t* Statistic: the absolute value for the *t* statistic >3.

The *t* statistic was calculated for the triplicate measurements of each gene on each array, using the log transformed ratios (*r*)

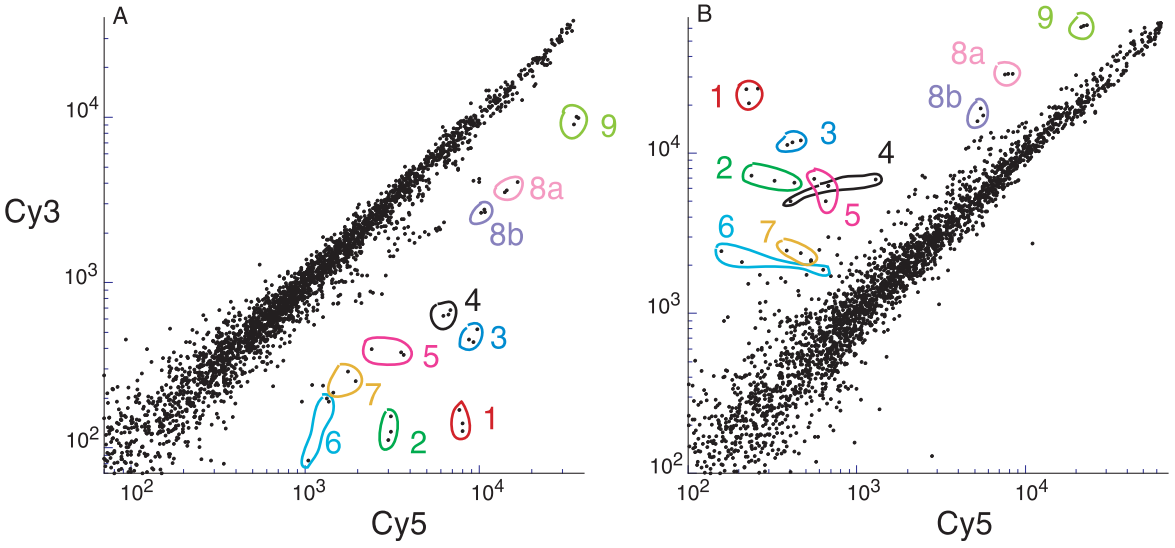

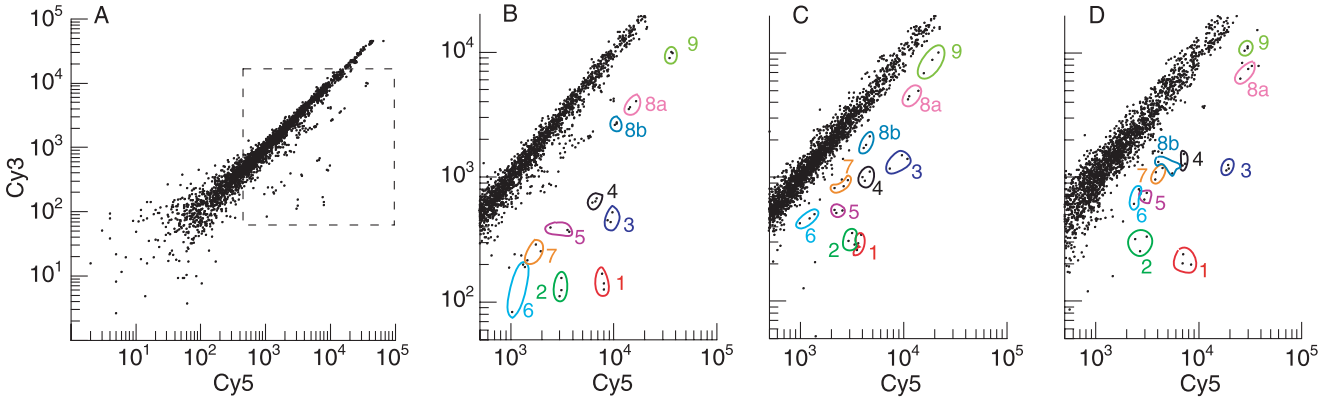

$$t = \frac{\bar{r}\sqrt{n}}{s}, \quad \text{where} \quad s = \sqrt{\frac{\sum_{i=1}^{n}(r_i - \bar{r})^2}{n-1}},$$

where $\bar{r}$ is the mean of the log transformed ratios, n is the number of measurement for each gene (3), and s is standard deviation of the three measurements for each gene.

(C) The signal intensity in at least one channel must be higher than 1% of the median signal intensity.

All array experiments included multiple independent sample comparisons. The complexity of the tissue source studied would determine the number of replicate experiments required to show differential expression before a transcript was considered for further study. For example, in a tissue of low complexity, such as a cell line, observing regulation in two of three experiments was accepted. All analyses were performed using a commercial spreadsheet program (Excel).

2.7.3. Calibration

It is widely recognized that microarrays underestimate the fold-change obtained for differentially expressed transcripts [7,8]. In statistical terminology, a consistent error in one direction is referred to as measurement bias. If this bias can be described by a function, it can be reduced by calibration. We investigated the bias of our cDNA microarray platform by using quantitative real-time PCR assays to provide the "gold standard" for comparison with microarray data [9]. This analysis demonstrated that the bias observed with cDNA arrays showed a power scale increase with increasing fold-change, causing a linear deviation of the log transformed data and the measurements could be corrected by the calibration function $F_c = F_{a(\mathrm{cDNA})}^{q}$, where $F_{a(\mathrm{cDNA})}$ is the microarray-determined fold-change comparing experimental and control samples, q is the correction factor, and F_c is the calibrated value.

3. Real-time PCR

The great value of microarrays lies in the large number of transcripts that can be assayed simultaneously. However, microarrays have several significant limitations. Microarrays require more RNA than quantitative real-time PCR (QRT-PCR). Errors in the identification of regulated transcripts (false positives and/or false negatives) depend on the threshold to identify a transcript as regulated as well as on the complexity of the tissue source (see below). Although some improvement is provided by the calibration algorithm described above, microarrays do not provide an accurate quantitative analysis of gene expression. Finally, the cost and effort involved in microarray assays introduces practical constraints in the number of RNA samples that can be analyzed, thereby reducing the number of replicate experiments and the statistical power of the results. These limitations can be largely overcome by incorporating high throughput real-time PCR into the study.

QRT-PCR provides reliable relative mRNA quantification over a large range of mRNA expression levels [10–12]. The accuracy of QRT-PCR combined with its potential for high sample throughput makes it an ideal complement to microarray analysis. After we identified candidate genes using the microarray platform described above, we performed independent confirmation experiments using QRT-PCR.

There are several different approaches to real-time PCR, including TaqMan assays [13,14] and molecular beacons [15,16]. We routinely utilize SYBR Green (Molecular Probes, Eugene, OR) detection of PCR products for real-time assays [17,18]. Real-time PCR relies on the quantification of PCR product during each amplification cycle via a change in fluorescence. Molecular beacons and TaqMan assays use a fluorescently labeled detection oligonucleotide. These approaches have the potential advantage of specificity. SYBR Green fluoresces when intercalated with dsDNA and will therefore detect any PCR product, including nonspecific products and primer-dimers. However, if the requirement for a single reaction product is imposed, SYBR green-based reactions provide specificity comparable to assays based on specific fluorescently labeled oligomers. In direct comparisons between TaqMan assays and SYBR green assays for the same targets, we found that SYBR green assays had comparable accuracy and provided more sensitivity (unpublished data). Furthermore, fluorescently modified probes

Fig. 4 (*Top*). Two-color overlay from raw TIFF files from one experiment. cDNA from GnRH treated LβT2 cells were labeled with Cy5, which appears red and cDNA from vehicle treated LβT2 cells were labeled with Cy3, which appears green. (A) Overview of the entire array. (B)–(D) Identical sections from three independent experiments. The bracket in each panel indicates an up-regulated gene (*egr1*) shown in triplicate spots. Reprinted from [5], with permission of the publisher.

Fig. 5 (*Middle*). Scatter plots of a dye reversal experiment. (A) cDNA from GnRH treated LβT2 cells was labeled with Cy5 and the cDNA from the control was labeled with Cy3. (B) cDNA from treated cells was labeled with Cy3 and the cDNA from control cells was labeled with Cy5. The triplicate spots from obvious regulated genes were encircled. In both panels are the same genes indicated by the same color.

Fig. 6 (*Bottom*). Scatter plots of independent replicate experiments where LβT2 cells were either treated with GnRH (Cy5 labeled) or vehicle (Cy3 labeled). (A) All data from one experiment are shown. Boxed area is enlarged in (B). (B, C) Scatter plots from three independent experiments. Triplicate spots from obvious regulated genes were encircled using the same color scheme as in Fig. 5. Reprinted from [5], with permission of the publisher.

are costly and take longer to synthesize than the standard oligonucleotide primers that are used for SYBR green assays.

3.1. Primer design

Primers were designed, whenever possible, within 1 kb of the polyadenylation site. Amplicons of roughly 100 bp were ideal but a length of 150–250 bp worked well. All primers were designed with the same T_m so that all reactions for any target could be run under standard conditions for the laboratory. The 3′ end of each 20mer primer was a G or a C and the G–C content was ~55%. The primers were screened for hairpins, priming on secondary binding sites within the target gene and dimer formation using a standard DNA analysis program, and for target specificity by BLAST (http://www.ncbi.nlm.nih.gov/BLAST). Primer pairs were tested for specificity by real time PCR followed by a dissociation curve and by agarose gel electrophoresis.

3.2. Real-time PCR

Real-time PCR requires the use of a specialized thermocycler with fluorescence detection capability. We used the ABI PRISM 7900HT (Applied Biosystems, Foster City, CA) configured to use 384-well plates and capable of unattended 24 h operation using a robotic arm to process plates in the queue.

For real-time PCRs, we used a previously described protocol [12]. Typically, 5 μg total RNA (as little as 0.5 μg was used for some assays) was transcribed into cDNA and 1/200 (approximately 500 pg) was utilized for 40 cycle three-step PCR.

We performed the real-time PCR in a 10 μl reaction volume

Volume	Component
2.3 μl	Deionized water
1 μl	PCR buffer 10× [200 mM Tris–HCl (pH 8.4), 500 mM KCl]
1 μl	$MgCl_2$ (50 mM)
0.05 μl	SYBR Green 1 (Molecular Probes, Eugene, OR), 100×[a]
0.2 μl	dNTPs (10 mM each)
0.4 μl	Primer mix (5 μM each)
0.05 μl	*Taq* DNA polymerase (5 U/μl) (Invitrogen, Carlsbad, CA)[b]
5 μl	Sample

[a] The 100× SYBR Green 1 is prepared by diluting 100 μl of the stock 10,000× concentrate into 10 ml of DMSO, then stored in 0.5 ml aliquots at −20 °C.

[b] "Hot start" Taq should be used. We used Platinum Taq (Invitrogen, Carlsbad, CA) for these assays.

Reactions were then placed in the thermal cycler and subjected to

95 °C for 2 min to activate enzyme[a]
95 °C for 15 s to denature
55 °C for 20 s to anneal
72 °C for 30 s to extend

Last three steps were repeated for a total of 40 cycles.

[a] Time will vary according to enzyme used.

3.3. Data analysis

The number of target copies in each sample was interpolated from its threshold cycle (C_T) value using a plasmid or purified PCR product standard curve included on each plate. The C_T value used for subsequent analysis was the median C_T observed with repeated measurements of each transcript.

The standard curve for *egr1* is shown in Fig. 7. In principle, the C_T values from a dilution curve for a perfectly efficient reaction should have a slope of −3.32. Although many laboratories use the linear slope of the C_T values plotted against DNA concentration to calculate efficiency, we found that this approach tends to overestimate reaction efficiency due to the reduction in efficiency associated with increasing amounts of template DNA. We found that it was preferable to calculate the efficiency of a specific PCR by an analysis of individual amplification plots using a mathematical model described elsewhere [9].

4. Organization of the early induced gene network

In this and the subsequent section, we describe several examples of the application of FMA to actual experiments. We used FMA to identify and characterize the rapidly induced gene network in a gonadotrope cell line in response to the hormone gonadotropin releasing

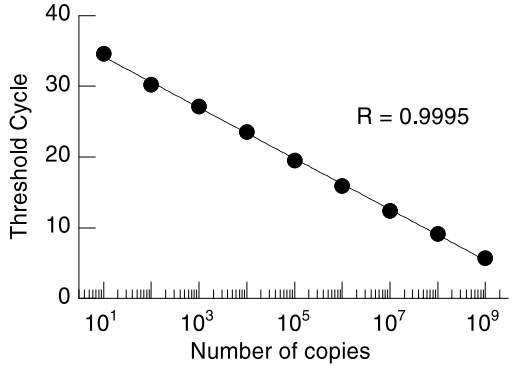

Fig. 7. Standard curve for real-time PCR. The standard curve for *egr1* transcripts is shown. Note the broad measurement range of the assay. Reprinted from [5], with permission of the publisher.

hormone (GnRH) [5]. The mouse LβT2 gonadotrope cell line was used for these studies [19]. The LβT2 cell line expresses the GnRH receptor and is a widely used model of the mouse pituitary gonadotrope, from which it was derived by targeted tumorogenesis [19]. Following GnRH receptor activation, a signaling cascade is initiated that leads to induction of transcription factors and, ultimately, regulation of the gonadotropin subunit promoters.

We utilized FMA in order to characterize the initial changes in gene expression that occur following GnRH exposure [5]. LβT2 cells were treated with 100 nM GnRH for 1h. RNA was extracted and analyzed by using the cDNA microarray (see Fig. 4). Because this experiment involved a homogenous cell line, we chose to perform only three replicate microarray experiments prior to follow-up QRT-PCR studies. Twenty-six genes were chosen for further analysis because they were identified as differentially expressed using the algorithm described above in at least two experiments. Twenty-three genes were confirmed to be regulated by QRT-PCR (Table 1). One hundred percent (17/17) of gene changes on the microarray with fold-changes >1.6 were confirmed. Sixty-six percent (6/9) of genes showing average changes between 1.3- and 1.6-fold on the microarray were also confirmed by QRT-PCR (Tables 1 and 2). In addition, we have found three genes which were not identified on the microarray, which were found to be regulated according to real-time PCR assays (see

Table 1
Fold-changes ± SEM from the early gene microarray compared to real-time PCR

Gene name	Accession Nos.	Microarray ($n = 3$) 1 h	SYBR PCR ($n = 9$) 1 h
LRG 21	U19118	**31.2 ± 16.6**	**96.8 ± 15.7**
Egr1	NM_007913	**12.9 ± 3.8**	**390.6 ± 83.9**
c-fos	J00370	**12.5 ± 4.0**	**52.0 ± 5.8**
Nr4a1/nur77	AI322974	**5.9 ± 1.5**	**49.4 ± 10.1**
Ier2/Pip92	W14782	**5.2 ± 1.2**	**17.1 ± 2.4**
Rgs2	NM_009061	**4.0 ± 1.3**	**8.7 ± 0.4**
c-jun	NM_010591	**3.8 ± 0.6**	**6.6 ± 0.9**
TSC22	NM_009366	**3.4 ± 0.4**	**3.3 ± 0.2**
γ-Actin	L21996	**2.7 ± 0.3**	**3.9 ± 0.4**
Klf-like EST	BE368139	**2.3 ± 0.3**	**2.5 ± 0.2**
Period1	AB030818	**2.1 ± 0.1**	**4.9 ± 1.1**
β-Actin	NM_007393	**2.0 ± 0.5**	**1.6 ± 0.1**
PRL1	NM_011200	**2.0 ± 0.4**	**2.1 ± 0.1**
IκB	NM_010907	**1.7 ± 0.2**	**2.6 ± 0.2**
Klf4	NM_010637	**1.7 ± 0.3**	**2.9 ± 0.3**
Gem	AA177829	**1.7 ± 0.2**	**4.3 ± 0.3**
Gly96	X67644	**1.7 ± 0.6**	**3.8 ± 0.5**
JunD	W12943	**1.6 ± 0.2**	1.2 ± 0.2
Egr2	AA727313	**1.5 ± 0.2**	**294.7 ± 35.6**
Transgelin	AF149291	**1.4 ± 0.1**	**1.8 ± 0.2**
NMDMC	NM_008638	**1.4 ± 0.3**	**1.6 ± 0.3**
Stat3B	U30709	**1.4 ± 0.2**	1.2 ± 0.1
MKP1/3CH134	W34966	**1.4 ± 0.1**	**3.4 ± 0.4**
Nrf2	U20532	**1.3 ± 0.2**	**1.5 ± 0.1**
HSP30	NM_019979	**1.3 ± 0.2**	**1.9 ± 0.2**
STY-kinase	M38381	1.3 ± 0.04	**1.7 ± 0.2**
Glucose transport protein	M22998	1.1 ± 0.4	**2.2 ± 0.4**
SCL	AJ297131	1 ± 0.2	**2.4 ± 0.2**
Gata2	NM_008090	*0.7 ± 0.1*	1 ± 0.1

Values meeting the criteria for up- or down- regulation are indicated by bold or italic, respectively. The identification of all clones listed was confirmed by sequencing. Modified from [5], with permission of the publisher.

Table 2
Summary of regulated gene confirmation in different experimental paradigms

Source	Arrays used	Gene candidates tested by PCR	PCR confirmed genes		
			All candidates	FC>1.6 on the array	FC<1.6 and >1.3
LβT2 cells	3	26	23 (88.5%)	17/17 (100%)	6/9 (66.7%)
Hypothalamus	5	16	12 (75%)	9/12 (75%)	3/4 (75%)
Cortex	7	14	4 (28.6%)	3/7 (42.9%)	1/7 (14.3%)

FC indicates fold-change. Reprinted from [21], with permission of the publisher.

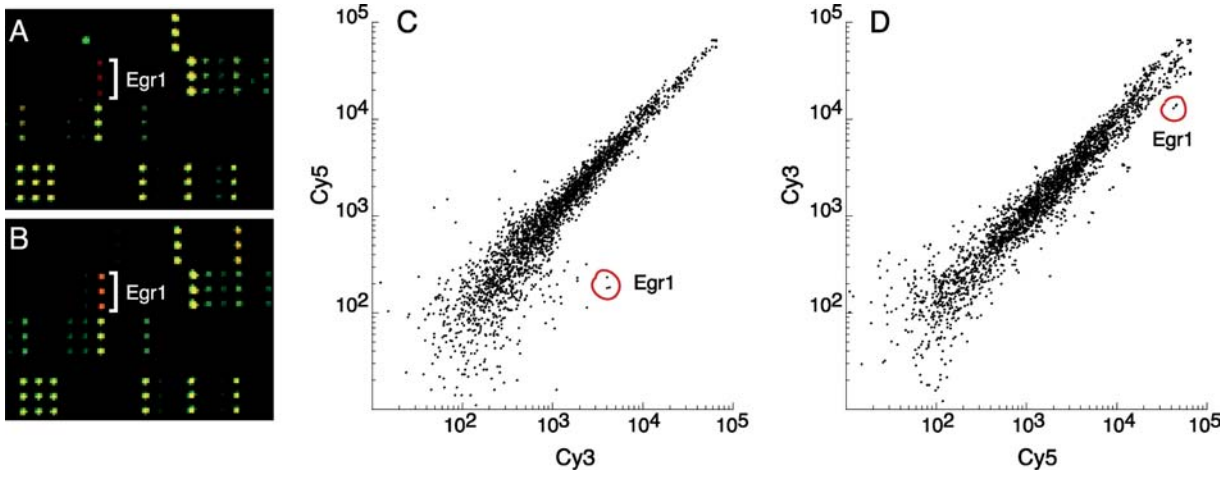

Fig. 8. Overlays and scatter plots comparing different concentrations of GnRH treatment. (A) Overlay and (C) corresponding scatter plot taken from 4 nM GnRH and vehicle treated LβT2 cells. (B) Overlay and (D) corresponding scatter plot taken from 4 and 100 nM GnRH treated LβT2 cells. Reprinted from [20], with permission of the publisher.

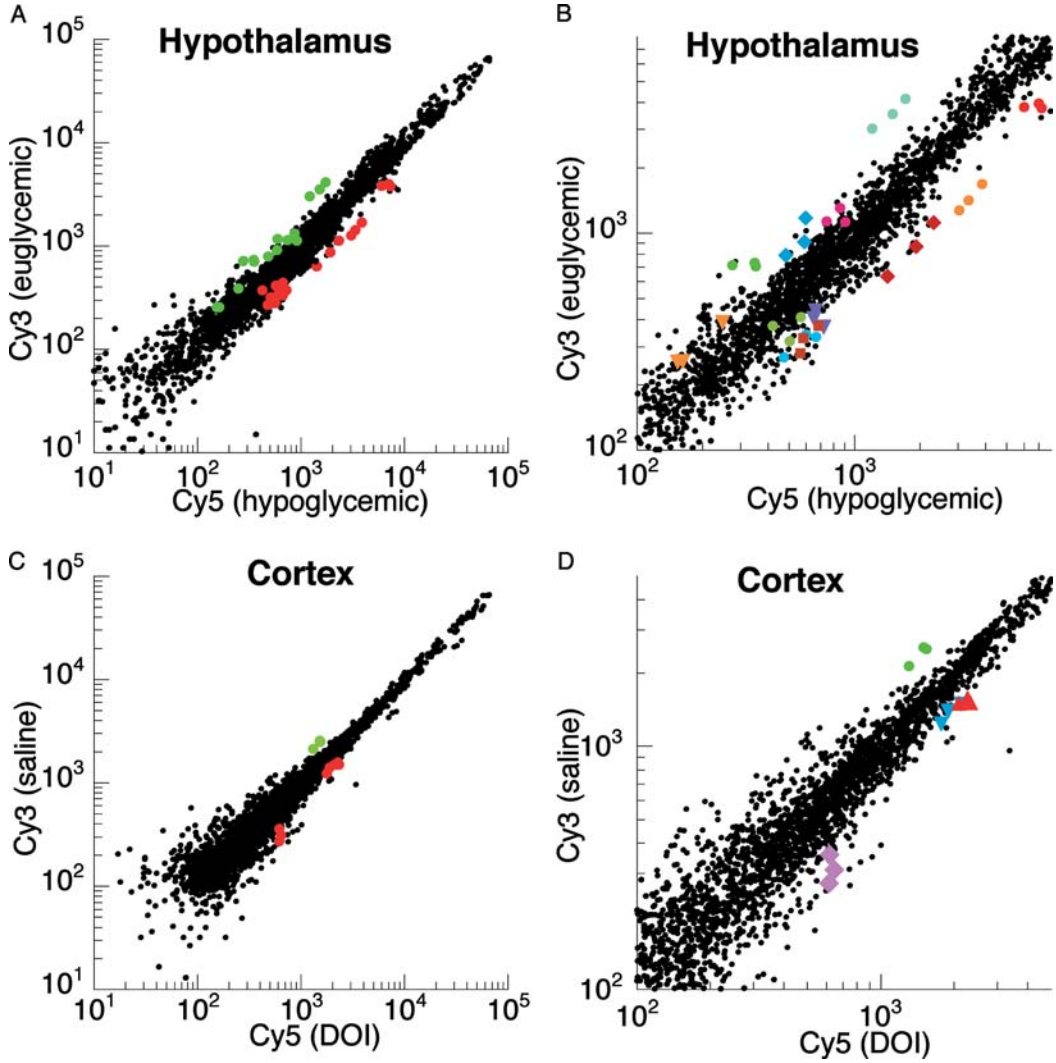

Fig. 9. Scatter plots of QRTPCR confirmed microarray assays from tissues with varying complexity. (A) and (B) Hypothalamic samples from euglycemic and hypoglycemic mice were compared. (C) and (D) Somatosensory cortex samples from DOI- and vehicle-treated mice were compared. (B) and (D) are enlarged section from (A) and (C), respectively. Regulated transcripts that were confirmed by QRTPCR assays are indicated in color. Modified from [21], with permission of the publisher.

Table 1). We were able to detect relative gene changes as low as 1.3-fold.

We also investigated the quantitative effects of GnRH concentration on the gene program induced. LβT2 cells were treated with either 4 nM GnRH or 100 nM GnRH for 1 h [20]. The microarray analysis could be used to efficiently screen genes that were differentially activated by different concentrations of GnRH (Fig. 8).

5. Complex tissues

The information contained in any gene assay is reduced by variations induced by measurement technique and by biological differences (even in samples from within the same treatment group). In a cell line, biological variation can be tightly controlled. We found in an analysis of variance that the biological variation among transcript levels in independent, replicated experiments was negligible in comparison with the measurement variation of the microarray assay itself [5]. In addition, as described above, microarray data from a cell line experiment can be highly accurate. In studies using animals or clinical samples, the biological variation is increased. This effect may be addressed by assaying RNA samples that are pooled from individual samples and/or by increasing the number of replicates studied.

Experiments in complex tissues introduce additional problems arising from the assay of heterogenous cell populations. Brain tissue, for example, contains a large number of different individual cell types. A particular experimental treatment might affect only a subset of these cells. Therefore, the level of change of any transcript in the RNA samples from that tissue is likely to be much lower than that observed in a homogenous tissue. In addition, any particular gene of interest may only be expressed in a small subset of cells, leading to a signal for that gene on the array that is difficult to measure reliably. These limitations are referred to as ''dilution effects'' [21]. We demonstrate in FMA studies of mouse hypothalamus and cortex that these theoretical limitations can be addressed in the experimental design, allowing the detection of transcripts showing low levels of change.

5.1. Hypothalamus

Regulatory changes in the hypothalamus that may contribute to hypoglycemia-associated autonomic failure in diabetics were studied. RNA was extracted from hypothalami of treated and untreated mice. In order to compensate for tissue complexity, a pooled design was used and five independent array assays were performed. Thus, 10 pools of RNA, each from four animals, were made: five pools from euglycemic (untreated) mice and five from hypoglycemic (treated) mice [21]. Further studies of candidate transcripts were done using QRT-PCR in samples from individual animals. Fig. 9 shows all QRT-PCR confirmed differentially expressed transcripts, indicated in color. As expected due to the dilution effect in hypothalamus experiments, no obviously regulated transcripts were apparent in the scatter plot (see Figs. 9A and B). The regulated genes were partly intermingled with non regulated genes in all microarray assays, although the triplicate measurements from each confirmed transcript were always displaced in the same direction (see Fig. 9B). The fold-changes ranged from 1.3 to 2.3 and the regulation of 12 of the 16 identified genes was confirmed by QRT-PCR (Table 2). These results demonstrate that although the gene changes in the samples were relatively low, the FMA approach was able to detect regulated genes.

5.2. Somatosensory cortex

To investigate the gene program activated by serotonergic hallucinogens in mouse somatosensory cortex, the effects of the 5-hydroxytryptamine 2A receptor agonist, 2,5-dimethoxy 4-iodoamphetamine (DOI) were studied. The 5-HT 2A serotonin receptor, a member of the G protein-coupled receptor superfamily, has a high level of expression in somatosensory cortex [22] and has been implicated in the effects of hallucinogenic drugs [23]. Mice were injected with DOI (treated) or vehicle (untreated) and sacrificed 1 h later. Somatosensory cortex samples were dissected for RNA extraction. Seven independent microarray hybridizations from seven different DOI- and vehicle-treated mouse pairs were performed [21]. The scatter plot of a representative microarray experiment is shown in Figs. 9C and D. Almost none of the genes showed obvious regulation. In all experiments the regulated genes were intermingled with unregulated genes. Four genes identified by the microarray could be confirmed by QRT-PCR. In these experiments, the percentage of genes identified by microarray which could not be confirmed by QRT-PCR was relatively high (see Table 2).

6. Concluding remarks

We described an optimized platform for genomics studies involving a defined, high quality microarray of restricted size, and extensive follow-up studies using QRT-PCR. Using this platform allowed the reliable and efficient detection of differentially expressed transcripts in a wide-range of experimental paradigms. We believe that elements of this approach are widely applicable to the structuring of experimental approaches using any microarray platform. The key elements of this approach include: (1) reduction of controllable variation in all aspects of the microarray experiment, (2) careful experimental design including repeated transcript

measurement on the microarray and adequate replication of the microarray experiments, and (3) complete and independent confirmation studies using high throughput QRT-PCR assays. The overall experimental design needs to be carefully adjusted for the experimental system and the experimental objectives. The results of the QRT-PCR validated experiments described above can be used as a guide for designing efficient and successful genomics experiments.

References

[1] A.J. Holloway, R.K. van Laar, R.W. Tothill, D.D. Bowtell, Nat. Genet. 32 (Suppl) (2002) 481–489.
[2] S.A. Bustin, S. Dorudi, Trends Mol. Med. 8 (2002) 269–272.
[3] G.A. Churchill, Nat. Genet. 32 (Suppl) (2002) 490–495.
[4] G.J. Kargul, D.B. Dudekula, Y. Qian, M.K. Lim, S.A. Jaradat, T.S. Tanaka, M.G. Carter, M.S. Ko, Nat. Genet. 28 (2001) 17–18.
[5] E. Wurmbach, T. Yuen, B.J. Ebersole, S.C. Sealfon, J. Biol. Chem. 276 (2001) 47195–47201.
[6] P. Hegde, R. Qi, K. Abernathy, C. Gay, S. Dharap, R. Gaspard, J.E. Hughes, E. Snesrud, N. Lee, J. Quackenbush, Biotechniques 29 (2000) 548–550, 52-4, 56 passim.
[7] M. Taniguchi, K. Miura, H. Iwao, S. Yamanaka, Genomics 71 (2001) 34–39.
[8] M.S. Rajeevan, D.G. Ranamukhaarachchi, S.D. Vernon, E.R. Unger, Methods 25 (2001) 443–451.
[9] T. Yuen, E. Wurmbach, R.L. Pfeffer, B.J. Ebersole, S.C. Sealfon, Nucleic Acids Res. 30 (2002) e48.
[10] N.J. Walker, J. Biochem. Mol. Toxicol. 15 (2001) 121–127.
[11] W.M. Freeman, S.J. Walker, K.E. Vrana, Biotechniques 26 (1999) 112–122, 24-5.
[12] T. Yuen, W. Zhang, B.J. Ebersole, S.C. Sealfon, Methods Enzymol. 345 (2002) 556–569.
[13] C.A. Heid, J. Stevens, K.J. Livak, P.M. Williams, Genome Res. 6 (1996) 986–994.
[14] T. Morris, B. Robertson, M. Gallagher, J. Clin. Microbiol. 34 (1996) 2933–2936.
[15] A.S. Piatek, S. Tyagi, A.C. Pol, A. Telenti, L.P. Miller, F.R. Kramer, D. Alland, Nat. Biotechnol. 16 (1998) 359–363.
[16] S.A. Marras, F.R. Kramer, S. Tyagi, Genet. Anal. 14 (1999) 151–156.
[17] C. Schneeberger, P. Speiser, F. Kury, R. Zeillinger, PCR Methods Appl. 4 (1995) 234–238.
[18] A. Becker, A. Reith, J. Napiwotzki, B. Kadenbach, Anal. Biochem. 237 (1996) 204–207.
[19] J.L. Turgeon, Y. Kimura, D.W. Waring, P.L. Mellon, Mol. Endocrinol. 10 (1996) 439–450.
[20] T. Yuen, E. Wurmbach, B.J. Ebersole, F. Ruf, R.L. Pfeffer, S.C. Sealfon, Mol. Endocrinol. 16 (2002) 1145–1153.
[21] E. Wurmbach, J. Gonzalez-Maeso, T. Yuen, B.J. Ebersole, J.W. Mastaitis, C.V. Mobbs, S.C. Sealfon, Neurochem. Res. 27 (2002) 1027–1033.
[22] J.F. Lopez-Gimenez, G. Mengod, J.M. Palacios, M.T. Vilaro, N. S. Arch. Pharmacol. 356 (1997) 446–454.
[23] R.L. Jakab, P.S. Goldman-Rakic, Proc. Natl. Acad. Sci. USA 95 (1998) 735–740.